

Association of Actin with Sperm Centrioles: Isolation of Centriolar Complexes and Immunofluorescent Localization of Actin

MAURICE G. KLEVE and WALLIS H. CLARK, JR.

Department of Animal Science, University of California, Davis, California 95616, and Department of Biology, University of Houston, Houston, Texas 77004

ABSTRACT The centrioles of cnidarian sperm associate with striated specializations (pericentriolar processes) during spermiogenesis. Three functions have been proposed for the role of these structures: (a) an anchoring mechanism for the sperm flagellum, (b) a signal-transmitting mechanism for communication between sperm head and tail, and (c) a contractile mechanism involved in motor function of the sperm flagellum. To investigate these proposed functions, we developed a technique for the isolation and purification of *Hydractinia* sperm distal centrioles with attached pericentriolar processes. SDS polyacrylamide electrophoretic profiles of whole sperm and pericentriolar process proteins revealed a prominent protein that comigrates with rabbit and penaeid shrimp muscle actin. To label and localize actin in hydroid sperm, we produced in rabbits a highly specific antiserum to invertebrate actin that cross-reacts with both invertebrate and vertebrate muscle and nonmuscle actin. Immunofluorescent double antibody labeling of hydroid sperm with antiactin has demonstrated the presence of actin in the pericentriolar process region of the sperm. In earlier reports, it has been proposed that pericentriolar processes, if contractile, could alter the mid-piece asymmetry of hydroid sperm, facilitating the directional motility that these cells demonstrate in response to egg-released chemoattractants. The present results support this hypothesis.

Striated specializations are common subcellular elements associated with centrioles and basal bodies in a great variety of cell types (27). The striated, myofibrillar-like appearance of these structures has led several investigators to suggest that they may be contractile in nature (13, 30). Recently, the calcium-dependent contractile nature of one such striated centriolar specialization, the rhizoplast of green alga, has been clearly demonstrated (29).

We have been working with the striated centriolar specializations (pericentriolar processes) associated with the distal centrioles of cnidarian sperm. For several years it has been recognized that cnidarian sperm respond to egg- or female-released chemoattractants. Two theories accounting for this behavior have been postulated. One opinion has been that alterations in the wave form of flagellar beat may be responsible for the directional selectivity of chemotactically stimulated sperm (18). Unfortunately, not all chemotactic sperm demonstrate these wave form alterations during turning (22). It has been proposed that the directed swimming of cnidarian sperm

may be attributable to a contractile mechanism associated with the distal centriole (3, 12, 13). Such a contractile mechanism would function to alter mid-piece symmetry, changing the angular relationship between sperm head and tail, giving the sperm a "rudder" capability. The hypothesis is based on several observations: (a) there appears to be a pronounced alteration in the head-tail angle during sperm turning (12); (b) cnidarian sperm distal centrioles are associated with striated pericentriolar processes, which, if contractile, are properly shaped and positioned to facilitate alterations in sperm mid-piece symmetry (3, 13); (c) centrioles and their associated specializations such as rootlets are capable of independent ATPase activity (1, 16, 30); and (d) as mentioned previously, such structures have now been demonstrated to be capable of contraction (29).

To increase understanding of the structure and function of pericentriolar processes and the role of distal centrioles in sperm motility, we have used two investigative approaches. First, techniques for the isolation of sperm distal centrioles with intact pericentriolar processes have been developed. Such

techniques are prerequisite to the molecular characterization of these structures. For this purpose we chose the hydrozoan, *Hydractinia echinata*, which possesses simple sperm we thought might lend themselves to disruption and organelle isolation. Second, keeping in mind that actin is generally accepted as a component of cellular and subcellular contraction, we have produced an antibody to invertebrate actin (14). Using indirect immunofluorescence microscopy with this antibody, we have specifically identified and localized actin in *Hydractinia* sperm.

MATERIALS AND METHODS

Acquisition of Sperm

Male colonies of *Hydractinia echinata* were collected and maintained on shells occupied by *Pagurus* sp. hermit crabs. The colonies were fed heavily on *Artemia nauplii* until full sexual maturation. During this period, the colonies were maintained under continuous photoexposure to prevent spawning. Mature colonies were spawned by exposure to an intense incandescent light source after a 12-h dark period (2).

Electron Microscopy

Whole gonophores containing late spermatids and mature sperm were fixed in Karnovsky's (11) glutaraldehyde-paraformaldehyde mixture buffered with 0.1 M phosphate. The tissue was dehydrated with acetone, embedded in epoxy resin (32), thin sectioned, and stained with lead citrate and saturated aqueous uranyl acetate.

Centriole preparations from the isolation procedure were applied one drop at a time to 0.4% Formvar-coated, carbon-reinforced grids. The excess fluid was removed with filter paper wicks, and the grids were stained with 0.2% aqueous uranyl acetate and air dried. These whole-mount preparations and the whole-tissue thin sections were observed on a Hitachi HS8 or AEI 6B electron microscope.

Centriolar Complex Isolation

Spawned sperm were washed with sterile artificial seawater and concentrated by sedimentation at 1,000 g. Pelleted sperm were suspended in a hypotonic buffer (SMT) containing 10 mM NaCl, 10 mM Mg₂SO₄, and 10 mM Tris-HCl (pH 7.2 at 0°C) at a cell concentration of 5×10^6 /ml. The sperm were allowed to swell for 10 min at 4°C. The suspension was then disrupted by 30 s of ultrasonication with a Bio Sonic Ultrasonicator set to mid-green range. The preparation was sedimented at 2,000 g and resuspended in SMT plus 0.02% Triton X-100 and sedimented again at 2,000 g. More than one sonication and detergent treatment may be required to separate the centriolar complex from other cell constituents. After the centrioles were properly detached, they were layered over 0.6 M sucrose buffered with SMT and cleared at 5,000 g for 30 min. The pellet was discarded, and the 0.6-M sucrose fraction was relayered over a step gradient of 0.6, 1.0, and 2.0 M sucrose and spun at 25,000 g for 30 min. Centriolar complexes that layered over the 2.0-M interface were recovered and prepared for electron microscopy and electrophoresis.

SDS Polyacrylamide Gel Electrophoresis

SDS polyacrylamide gel electrophoresis was performed according to Weber and Osborn (38). Standard 10% acrylamide, 3.5% bisacrylamide gels were run at 8 mA per gel for analysis of protein purity and molecular weight determination. Protein samples were dissolved in sample buffer containing 0.1 M sodium phosphate, pH 7.2, 2% SDS, 1% β -mercaptoethanol (MEO), 15% glycerol, and 0.002% bromophenol blue marker dye. To facilitate dissolution, some samples were heated to boiling for 2–4 min with the addition of 8 M urea to the sample buffer. The SDS running buffer contained 0.1 M sodium phosphate, pH 7.2, and 0.1% SDS. Gels were stained in 0.1% Coomassie Blue R 250, 50% methanol, and 10% acetic acid at 50°C at 2 h. Destaining was conducted overnight at 50°C in 400 vol of 7% methanol, 7% acetic acid with two changes. Densitometric measurements of protein levels in SDS electrophoresis bands were made on a Canalco Model G scanning densitometer with yellow filters (560 nm). Each disc gel was scanned three times with 120° rotation between scans, and the resulting peaks were integrated to give the composite scans presented here.

Antibody Production

A detailed description of the antibody production technique, including the purification of antigen and the muscle marker proteins used for electrophoresis,

is described elsewhere (14). In brief, invertebrate muscle actin was obtained from penaeid shrimp tail muscle and was purified by self-assembly polymerization (31) and SDS gel electrophoresis (15). The antibodies were produced in rabbits and partially purified from sera by ammonium sulfate precipitation. The antibody cross-reacted specifically with native, SDS-denatured, or formalin-fixed actin and gave double immunodiffusion precipitin reactions at a 500-fold dilution of sera.

Indirect Immunofluorescence

Spawned sperm were fixed for 20 min with 3% formaldehyde in phosphate-buffered saline (PBS). The fixed sperm were smeared and air dried on coverslips, treated with -10°C acetone for 7 min and washed for 1 min in PBS. The coverslips were then incubated for 45 min at 37°C in ammonium sulfate-precipitated antipenaeid-actin globulins diluted 1:50 with PBS. After four 10-min washes in PBS, the sperm-coated coverslips were incubated for 45 min with fluorescein-conjugated goat IgG (prepared against rabbit IgG) diluted 1:6 with PBS. After four additional 10-min washes in PBS, the coverslips were mounted on glass slides in a drop of 1:1 glycerol:PBS, pH 9.5–10.0. Controls were treated as were experimentals, except that preimmune rabbit globulins or actin-absorbed antipenaeid globulins were used. A series of incubations was conducted with PBS dilutions of antibody ranging from whole serum concentration to 1:500 dilution. The 1:50 dilution with PBS gave the most acceptable fluorescence for photographic purposes. No detectable difference in fluorescence pattern was noted over the range of the dilution series.

RESULTS

Pericentriolar Process Structure

The pericentriolar process complex is composed of nine processes that emanate from the distal centriolar matrix between the triplets (Fig. 1). Each of the nine members is composed of a primary process that extends from the centriolar matrix for $\sim 200 \mu\text{m}$ and terminates in a thickened tip. Three secondary processes radiate from that tip, also extending 200 μm and terminating in thickened tips. Numerous tertiary elements extend from the tips of each secondary process. Interprimary processes are components that interconnect adjacent primary processes. They are positioned diagonally with respect to primary processes and extend from the base of one primary process, near the point of matrix attachment, to a point near the thickened tip of the next primary process. Interprimary processes are parallel to the plane of centriolar triplet blades, while primary processes are perpendicular to the blades. The

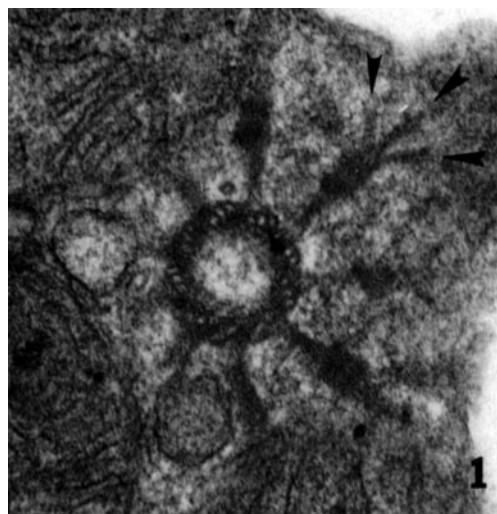


FIGURE 1 Cross section of the posterior region of a late spermatid. The section passes through the distal centriole at the level of the pericentriolar processes. Nine primary processes can be seen emanating from the centriolar matrix between triplets. The primary processes terminate in thickened tips, and three secondary processes emanate from these tips (arrows). $\times 56,000$.

entire complex extends radially from the centriolar matrix into the sperm cytoplasm between the mitochondria and plasma membrane, where it lies in close apposition to the membrane. Thus, the elements of the pericentriolar process complex form a cradle that wraps around the mitochondria of the sperm mid-piece, often extending anteriorly until they meet the nuclear envelope (Fig. 2).

In thin section, both primary and secondary processes appear to be composed of parallel longitudinal filaments with a subunit diameter of 50–70 Å. Primary and secondary processes appear striated, while interprimary processes are composed of parallel filaments that do not demonstrate a striated periodicity. The striations consist of a minor banding pattern covering the length of primary and secondary processes and major bands that occupy thickened positions midway down the length of processes and the thickened tips that terminate processes. The minor band striations, which appear as alternating light and dark transverse bands, are not generated by periodic changes in filament arrangement, packing, or subunit diameter. In advantageous sections that show separation of the filaments, it can be seen that the dark minor bands are composed of a dense material that transverses and connects the longitudinal filaments (Fig. 3). The pericentriolar processes are thus composed of units of longitudinal filaments and minor transverse bands that are bounded by high-density major bands. Each unit is composed of seven to ten sets of light and dark minor bands, with primary and secondary processes being composed of two to three such units. It cannot be determined from thin-section material whether the longitudinal filaments terminate at the point of insertion into minor or major transverse bands, or run as continuous filaments over the total length of each process.

In fixed material the spacing of striations is somewhat variable, ranging from 100 to 200 Å for the light bands and from 50 to 100 Å for the dark bands. It also appears that as the width

of light bands decreases, the width of dark bands increases. The major bands that separate blocks of minor band units are ~200–300 Å wide and are ~100 μm apart.

The array of pericentriolar processes forms an extensive and intricate complex. A detailed ultrastructural description of the centriolar complex and pericentriolar processes of cnidarians has been presented in previous studies (3, 13). For the sake of clarity, a schematic diagram of the distal centriolar complex of *Hydractinia* sperm is presented in Fig. 4. This gives a concise picture of the spatial relationship of the various components of the centriolar complex.

Isolation Procedure

Successful isolation of *Hydractinia* distal centrioles with attached pericentriolar processes is dependent on the extent of swelling and the duration and extent of sonication. There were two major objectives in the swelling procedure: (a) to expand the cytoplasm of the sperm, causing turgor on the plasma membrane, thus making the membrane more susceptible to fracture by ultrasonication; and (b) the disruption and dislocation of the internal sperm organelles (mitochondria, nucleus, and flagellum with attached centriolar complex).

The swelling treatment appears to have little effect on the nucleus, which does not swell with respect to the cytoplasm. The nucleus does, however, become loose and floats freely in the cytoplasm (Fig. 5). During swelling, the mitochondria are dislodged from their posterior position at the base of the nucleus and also float freely in the cytoplasm. The flagellum is drawn into the sperm cell and wraps itself around the cell periphery. Such loosening of the sperm's internal components is perhaps responsible for the intact state of the delicate pericentriolar processes after isolation.

The first sonication accomplished the disruption of the sperm

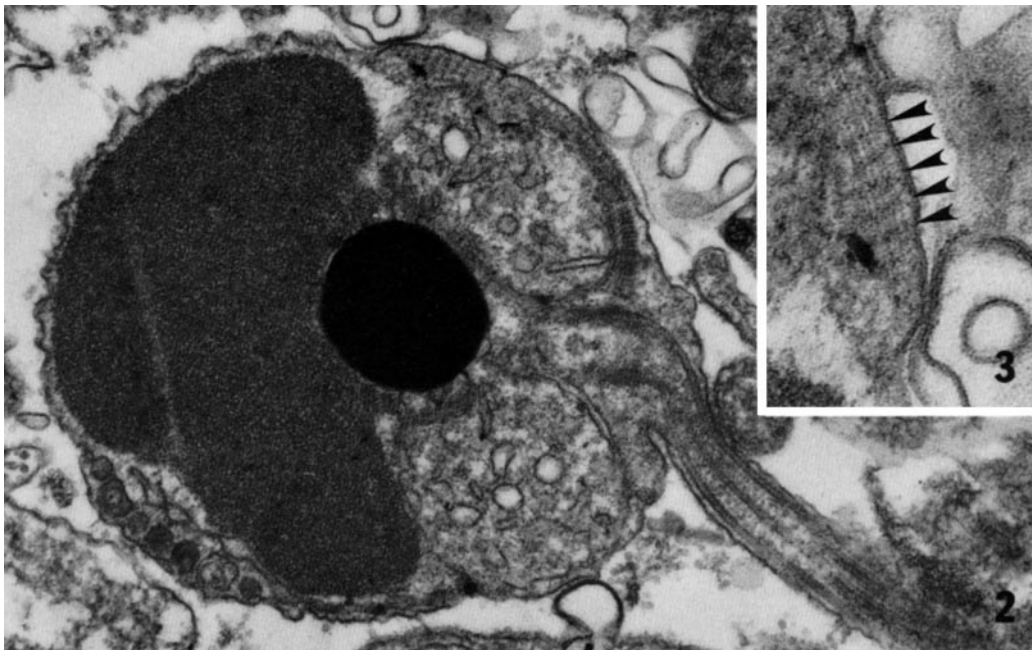


FIGURE 2 Longitudinal section passing through the mid-plane of a late spermatid. The pericentriolar processes that emanate from the distal centriole are clearly striated. They run between the plasma membrane and mitochondria and extend in an anterior direction to the nuclear membrane and form a cradle around the sperm mid-piece. $\times 36,000$.

FIGURE 3 High magnification of pericentriolar processes shown in Fig. 2. In this advantageous section the 50-Å filaments that run longitudinally along the process are visible as well as the dense material that transverses these filaments to give the processes their striated appearance (arrows). $\times 150,000$.

plasma membrane, producing a bray of cellular components. The centriolar complex remains attached to the flagellum and some adhering cytoplasmic matrix. The detergent treatment detaches the centriolar complexes from flagella and removes the cytoplasmic matrix. Centrifugation into 0.6 M sucrose eliminates most of the cytoplasmic contamination, and the final sucrose step gradient concentrates the centriolar complexes and separates them from axonemal fragments. Repetition of the differential sedimentation step and pooling of several runs will yield centriolar complexes of good quality in sufficient amount (100 μ g or more) for biochemical analysis.

Figs. 6 and 7 are whole-mount electron micrographs of

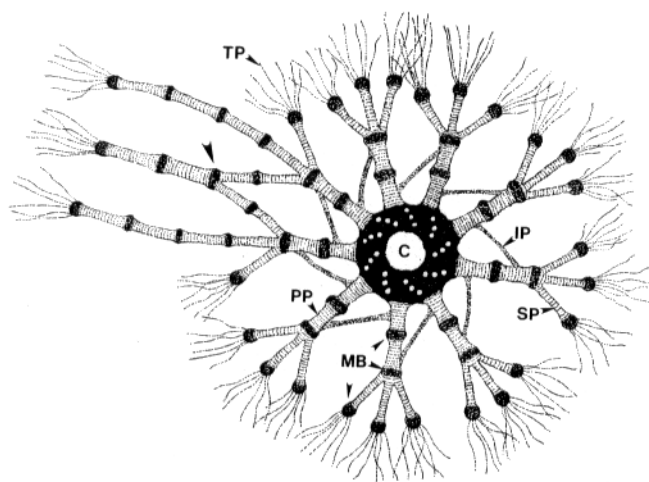


FIGURE 4 A cross-sectional schematic of the distal centriolar complex of *Hydractinia* sperm depicting the pericentriolar process array. The prominent components of the complex are the dense distal centriolar (C), nine primary processes (PP), 27 secondary processes (SP), filamentous tertiary processes (TP), and the interprimary processes (IP) that connect adjacent primary processes. The thickenings that appear along primary and secondary processes are major striated bands (MB) which correspond in dimensions with the major bands of striated ciliary rootlets. Two of the four long secondary processes, which give the complex asymmetry, fuse to form one process at their second major band (arrow).

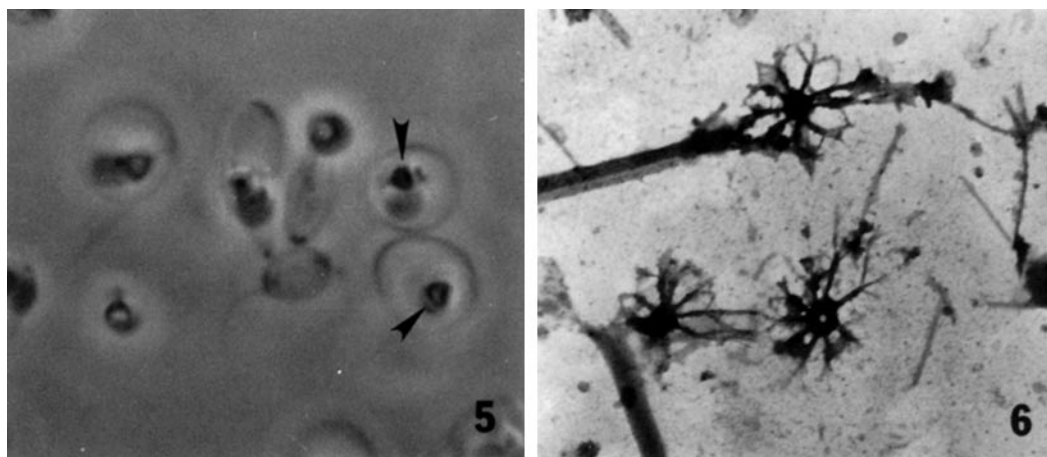


FIGURE 5 Phase-contrast micrograph of hydroid sperm subjected to swelling with hypotonic buffer. As is typical of swollen sperm, the tails are drawn into the cell body. During the swelling procedure, mitochondria and the sperm nucleus are frequently separated and float freely in the extended cell cytoplasm. Often the mitochondria also swell and rupture before the ultrasonication treatment. Sperm nuclei appear unaffected by the swelling procedure (arrows). $\times 1,500$.

FIGURE 6 Whole-mount electron micrograph showing the typical appearance of isolated distal centrioles with their pericentriolar processes attached and intact. This micrograph was selected to show the maximum level of contamination. As can be seen quite often, the centrioles also remain attached to fragmented portions of the sperm flagellum. $\times 12,500$.

isolated centriolar complexes. Pericentriolar processes are well preserved in the isolation procedure. These structures demonstrate extraordinary stability during isolation and are easily stored frozen without apparent structural degradation. They retain their primary and secondary processes ending in thickened tips; however, tertiary elements are for the most part lost in the isolation procedure. The minor band striations appear in whole mount as a negative image of that seen in sectioned material. Because the uranyl acetate staining procedure used in these preparations is a positive rather than negative stain, these results are confusing. The major bands that separate the seven- to ten-unit blocks of minor bands are not negatively stained by the procedure and appear much as they do in sectioned material.

In whole mount, the isolated process complex appears to be asymmetrical, an aspect poorly discernible in thin section because of the angle of process projection from the centriolar matrix. This asymmetry is demonstrated by the secondary extensions of two adjacent primary processes. These are much longer than those extending from the other seven (Fig. 7). In whole mount, it is clear that these long, secondary processes anastomose at their extremities, while the other seven sets of processes are unconnected except for the interprimary processes. Centriolar complexes viewed in isolates and thin sections from early spermatids do not demonstrate this asymmetry and fusion, which is observed only as the sperm approach maturity (13).

Electrophoresis of Distal Centriolar Proteins

The electrophoretic distributions of whole sperm, centriolar isolate proteins, and muscle protein markers are shown in Fig. 8. The electrophoretic profile of whole-sperm extract (Fig. 8 B) is complex, with the large number of low-level protein bands that would be expected from a whole-cell extract. Both actin- and tubulin-comigrating proteins are clearly present in whole sperm. These sperm proteins comigrate identically with control actin and tubulin on both comparative and actin-tubulin spiked gels. The centriolar isolate gel (Fig. 8 D) differentiates numerous protein bands, the most prominent of which comigrate with control tubulin (55,000 daltons) and actin (42,000 daltons).

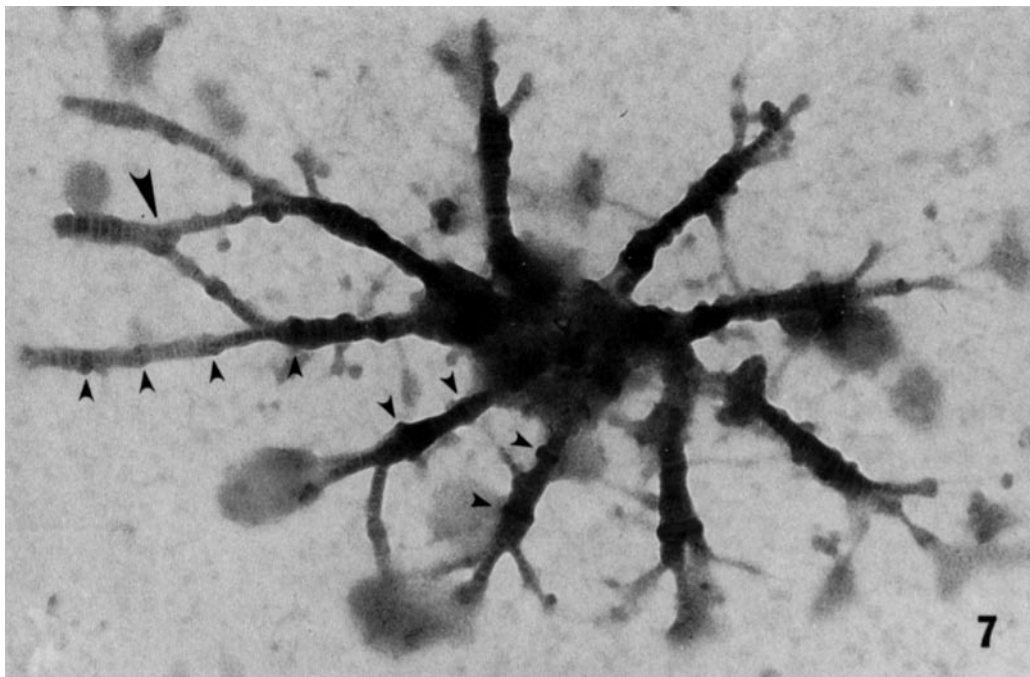


FIGURE 7 High-magnification whole-mount electron micrograph of an isolated distal centriole with particularly well-preserved pericentriolar processes. The striated banding of the processes can be seen and the mid-process thickenings which are comparable to major bands of striated rootlets are clear (small arrows). The asymmetry of the complex is demonstrated by the two long secondary processes and the point of anastomosis between these processes is marked by a large arrow. $\times 80,000$.

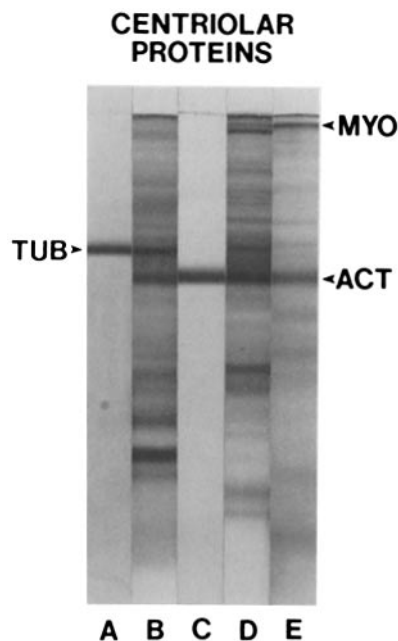


FIGURE 8 SDS electrophoretic profiles of whole sperm, centriolar extract, and contractile marker proteins. All gels were 10% acrylamide and were run for molecular weight determination. Gel A was run with purified bovine brain tubulin, gel B contains a total protein extract of whole washed hydroid sperm, gel C contains purified shrimp tail muscle actin, gel D contains a total protein extract of isolated distal centrioles with intact pericentriolar processes, gel E contains a rabbit muscle extract with enriched quantities of myosin and actin. Both whole sperm and centriolar isolate extracts contain proteins which comigrate with tubulin and actin.

Densitometric scans of centriolar isolate and whole-sperm gels are shown in Fig. 9. Expectedly, the densitometric scan of whole sperm indicates that the tubulin-comigrating band is the most plentiful single protein present. The scans of centriolar

isolate proteins indicate that actin-comigrating protein is the most prominent protein found in the centriolar fraction of hydroid sperm. This enrichment of actin-comigrating protein associated with the centriolar fraction containing pericentriolar processes suggests that a majority of this protein present in *Hydractinia* sperm is associated with the centriolar region.

Antiactin Labeling of Sperm

The fluorescent labeling pattern observed in *Hydractinia* sperm treated with antiactin forms a cradle surrounding the mid-piece mitochondria (Fig. 10). This fluorescence extends from the distal centriole anteriorly to the nuclear region of the sperm overlaying the area occupied by the pericentriolar process complex. In well-labeled sperm, stronger fluorescence can be seen running in longitudinal bands from the centriole to the nucleus. The distal centriole proper also demonstrates intense fluorescence with antiactin treatment. This pattern follows the positioning of pericentriolar processes as depicted in the schematic diagram shown in Fig. 11. No significant labeling was seen at the anterior end of *Hydractinia* sperm that do not possess an acrosome (8). Sperm treated with antiactin demonstrate no significant tail labeling as seen in mammalian sperm that have been tentatively demonstrated to contain actin (36). Control sperm were treated with ammonium sulfate precipitates of preimmune sera or immune sera adsorbed with purified actin. Under these conditions, *Hydractinia* sperm do not fluoresce.

DISCUSSION

Location of Actin in the Centriolar Complex

Three lines of evidence have been presented to verify the presence of actin in the centriolar complex of *Hydractinia* sperm. The structural observations of pericentriolar processes indicate that these structures are composed of parallel longitudinal filaments with a diameter similar to that of actin

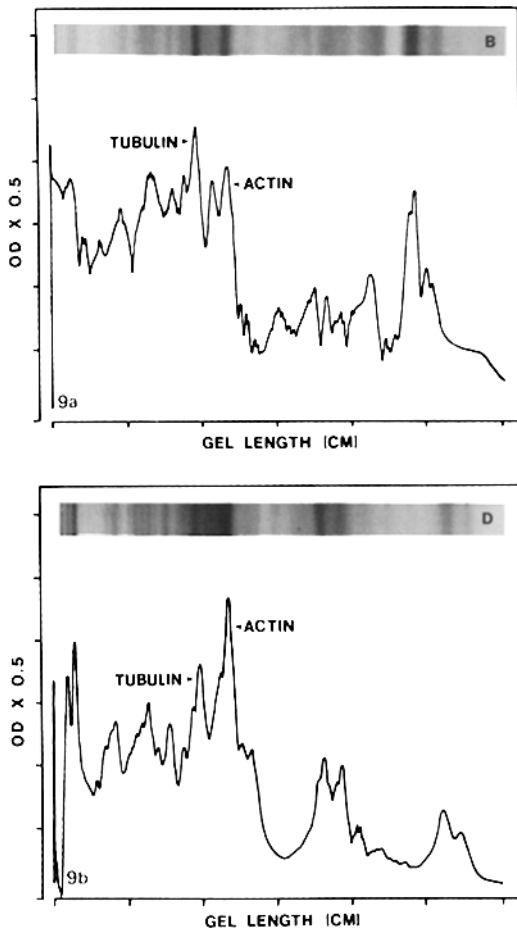


FIGURE 9 A comparison of optical density scans of tubulin- and actin-comigrating proteins from whole sperm and centriolar isolates run on SDS polyacrylamide gels. (a) The scan of gel B in Fig. 8 containing whole sperm proteins. (b) The scan of gel D in Fig. 8 containing centriolar isolate proteins. The change in ratio of actin to tubulin between whole sperm and sperm centrioles is more than one optical density unit. This change in ratio between actin and tubulin indicates that the centriolar fraction is actin rich when compared to the total sperm. The reversal of actin-tubulin ratio found in isolated centrioles is significant when the tubulin (axone-mal) contamination of centriolar isolates is considered.

microfilaments. SDS electrophoresis of whole sperm and isolated distal centriolar complex peptides indicates the presence of a protein with a molecular weight identical to that of actin monomer. The densitometric analyses of SDS gel profiles of whole sperm and isolated centriolar complexes cannot be compared quantitatively, because the weight fraction of centriolar complexes with respect to whole sperm cannot be determined. Qualitatively, however, the enrichment of the centriolar complex fraction with actin-comigrating protein is apparent. Double-antibody immunofluorescent-labeling experiments with specific antibodies to actin indicate that the distal centriolar complex contains a protein immunologically identical to actin. From these lines of evidence, it is our conclusion that the distal centriolar complex contains actin.

The immunofluorescence data presented here suggest that both the pericentriolar processes and the distal centriole proper probably contain actin. The structural observations of the filamentous nature of the pericentriolar processes suggest that actin is arranged in microfilaments that extend longitudinally along the process arms. These microfilaments may be maintained in the organized structure of the pericentriolar processes by cross-linking material that gives the process complex its striated appearance. Another study has tentatively localized a protein immunologically like actin in the striated basal feet of ciliary basal bodies (7). In this case, the majority of the actin was localized in the dark portion of the striated banding and in the dense matrix that connects the basal foot and centriole. The organization of actinlike protein in the distal centriole, which does not demonstrate a filamentous nature aside from the microtubular triplets themselves, is not clear. Perhaps this protein is present as a component of the extensive distal centriolar matrix. This matrix is not present in proximal centrioles, which do not label with antiactin.

Contractile Nature of the Centriolar Complex

The variability of band width and separation seen in pericentriolar process striations suggests that, if contractile, these processes may function in a fashion similar to that proposed for rhizoplasts (29). In rhizoplasts, the shortening of the filamentous portion of the striated unit is accompanied by a lengthening and thickening of the dense amorphous striations that transverse the rhizoplast. This would explain the high

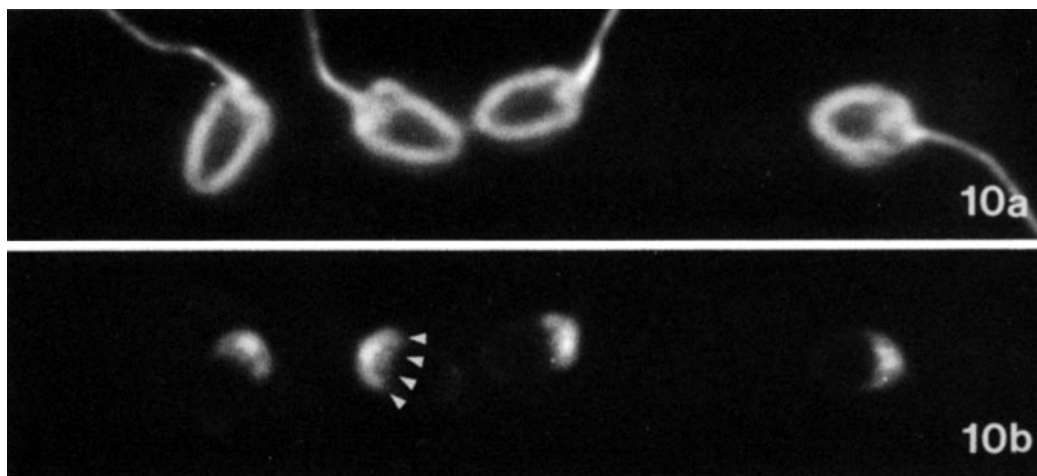


FIGURE 10 UV and tungsten light micrographs of antiactin-treated *Hydractinia* sperm. (a) Image of four sperm with dark-field tungsten illumination to aid in visualization of the sperm outline for reference. (b) UV image of the same four sperm shown in a. The fluorescent pattern demonstrates antiactin labeling in the region occupied by the pericentriolar process complex. Note the longitudinal zones of intense fluorescence which correspond to the position of pericentriolar processes (arrows). $\times 4,200$.

degree of variability in striated band width seen in the pericentriolar process complexes, some of which may have been stopped, by fixation, in the process of contraction, while others were relaxed. Similar variations in the striated pattern of ciliary rootlets have been observed and suggested to represent a possible contractile process (30). The structural data presented here, although not precluding a sliding filament mode of contraction, tend to support a system of filament rearrangement such as assembly-disassembly. In such a system, the dense, dark bands may act as areas of storage for depolymerized components such as G-actin and as sites of attachment and nucleation for the filamentous components such as F-actin, which may represent light bands.

Although variations in Ca^{++} level cause contraction of the algal rhizoplast *in situ* (29), preliminary experiments that introduced various divalent cations and phosphonucleotides to isolated centriolar complexes from *Hydractinia* sperm have not generated measurable contractions. Undoubtedly, the isolation procedure used in this study for acquiring distal centriolar complexes causes the loss of many soluble complex components, some of which may be required for contractile function.

Several fundamentally difficult questions must be answered before a model for contraction can be seriously proposed. The exact location, within the pericentriolar process complex, of contractile proteins such as actin must be determined at the electron microscope level. The existence and location of energy-liberating mechanisms such as myosin ATPase and other regulatory proteins such as tropomyosin and troponin need to be determined, and ultimately a successful *in vitro* system in which contraction can be studied must be developed.

Role of the Centriolar Complex in Sperm

Previous investigators have suggested three possible roles for striated rootlets, including pericentriolar processes that are

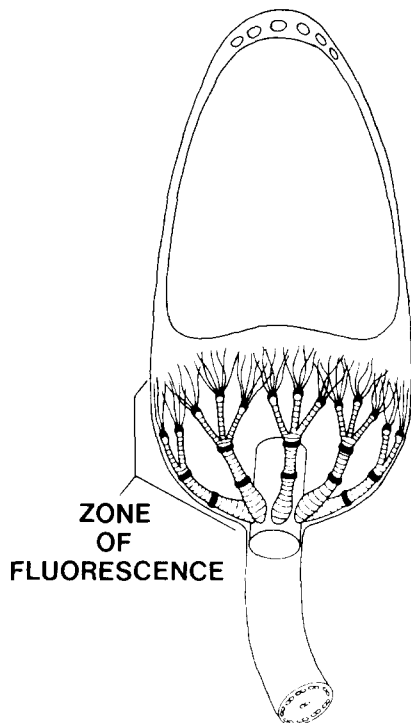


FIGURE 11 Schematic diagram of *Hydractinia* sperm showing the location of the pericentriolar process complex that forms a cradle around the sperm mid-piece and the area of antilactin localization with respect to pericentriolar process location.

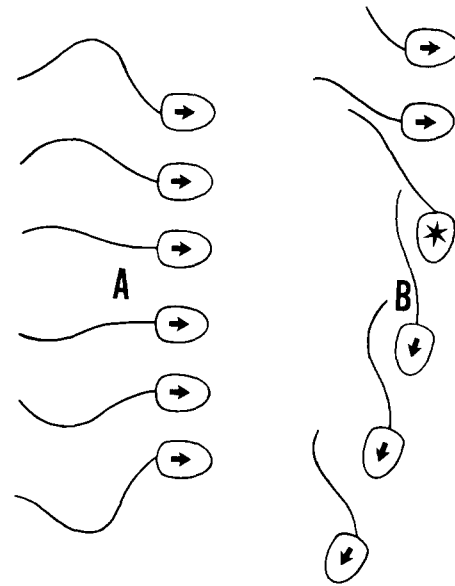


FIGURE 12 Schematic diagram of proposed model for hydroid sperm turning under influence of chemo-attractants. Part A represents the pattern of tail wave form and relationship of head-tail alignment during nonchemotactic swimming. Part B represents the pattern of tail wave form and relationship of head-tail angle during chemotactically induced sperm turning. The change in head-tail angle which is simultaneous with the change in sperm swimming direction is marked with a star.

associated with centrioles or flagellar basal bodies. One of these possibilities is that striated rootlets are structural, acting as an anchoring mechanism to absorb the energy generated by flagellar or ciliary motion (3, 9, 33-35). Another possible role is sensory, providing a signal-transmitting network in specialized cells with sensory cilia (6, 16, 34). The third suggested function is contractile, participating in motor function and flagellar or ciliary movement (3, 13, 30). The contractile role is particularly appealing to us, considering the recent evidence of contractile function (29) and the clearly demonstrated directional selectivity of chemotactically stimulated sperm (22).

The most obvious chemotactic sperm behavior is seen in cnidarian species including *Hydractinia* (20, 26). The cnidarian species, which demonstrate a high level of directional selectivity, also possess elaborate pericentriolar processes. It is interesting to note that species such as the sea urchin that do not express chemotactic behavior also do not possess striated centriolar specializations. Alterations in the sperm mid-piece symmetry resulting in a change in the angle of flagellar projection would provide the rudder necessary for this directional selectivity. A contractile unit located at the base of the mid-piece and preferably attached to the distal centriole and flagellar shaft could provide the motive force necessary to change either the mid-piece symmetry or the angle of flagellar shaft projection from the sperm mid-piece. Because of the location and structural form of the pericentriolar processes, we believe that this complex may serve such a contractile function.

The second alternative, that of a sensory or signal-transmitting mechanism, is also appealing. When sperm respond to a chemoattractant, they are functioning as a single-cell sensory unit. In such an instance, the sperm flagellum may be functionally analogous to a sensory cilium. Numerous investigators have observed pericentriolar process complexes associated with the basal bodies of sensory cilia. Pericentriolar processlike structures are found in the sensory cilia of the vertebrate inner

ear and lateral line organs (4, 5, 39), olfactory cilia (28), and photoreceptive cilia (10, 37). The role that pericentriolar processes play in the function of sensory cilia is not clear. These cilia are not involved in locomotor activity and do not seem to require an anchoring mechanism to support flagellar motion. Their frequent association with sensory cilia as opposed to locomotor cilia, however, implies a functional connection. In the case of sensory cilia, pericentriolar processes may orient the ciliary shaft toward the stimulus. The pericentriolar processes of chemotactic sperm may serve both locomotor and sensory roles.

The directional selectivity expressed by cnidarian sperm presented with a chemoattractant of female origin consists of two phases: the reception and recognition of the stimulus, and the response to that stimulus. The understanding of both phases is still quite limited. With respect to the first phase, our knowledge of sperm receptor site location, the mode of signal recognition of those sites, and the mechanism of signal transmission to the point of second phase action is only conjecture. There is, however, some knowledge of the nature of the chemotactic substance and the substance's general effect on sperm (17, 19, 21–26). The attractant appears to be a small peptide (under 1,000 daltons) that is species specific, protease labile, and requires calcium in the medium (seawater) to affect sperm. The attractant appears to provide a differentiable signal to the sperm by a concentration gradient that the sperm follows.

When presented with chemoattractant, hydroid sperm undergo obvious behavior changes that may relate to the second phase of the chemotactic reaction. Treatment of sperm with attractant has a complex effect on the mode of swimming. Flagellar beat rate and wave amplitude increase, and the nature of swimming (straight line as opposed to circular) is altered. This change in flagellar movement is characterized by a suppression of the flagellar wave form over the posterior half of the flagellum and an asymmetry in the wave form over the anterior half. These alterations cause the flagellar beat to have a wave of large amplitude and low radius, with the concave margin of the wave in the direction of the turn being made by the sperm (22, 25). The change in angle of flagellar projection is different during chemotactic turning. In this case, the change in angle is completed before the termination of the wave as would be the case with normal swimming. The actual change in angle occurs at the initiation of the new wave and causes, or is at least simultaneous with, the change in sperm swimming direction. We have proposed a hypothetical model (Fig. 12) summarizing these events as they relate to sperm directional swimming.

Our interpretation of the mode of directional turns made by sperm in response to a chemoattractant implies the presence, in the posterior mid-piece of the sperm, of contractile units that can change the orientation of the distal centriole and the flagellar shaft with respect to the sperm head. This interpretation is substantiated by the data presented in this study, indicating that the pericentriolar processes are associated with the distal centriole and the flagellar shaft; that pericentriolar processes are situated in an appropriate position to mediate changes in centriolar and flagellar orientation; and that actinlike proteins are associated with the pericentriolar process complex. This interpretation is further supported by recent studies showing: the contractile nature of other striated centriolar specializations (29), the involvement of calcium in both the process of centriolar specialization contraction (29) and sperm chemotaxis

(21), and the presence of ATPase in the striated specializations of centrioles (1, 16).

The authors wish to thank Drs. Luther E. Franklin (Department of Biology, University of Houston, Houston, Tex.) and John W. Fuseler (Department of Cell Biology, University of Texas, Health Science Center, Dallas, Tex.) for the contribution of their time and facilities during this study. We also wish to thank Dr. Cadet Hand at the University of California, Bodega Marine Laboratory (Bodega Bay, Calif.), for his thoughtful comments and review during the preparation of this manuscript and Ann McGuire for her editorial comments.

Supported in part by Sea Grant 04-3-158-18.

Received for publication 17 September 1979, and in revised form 15 February 1980.

REFERENCES

- Anderson, R. G. W. 1977. Biochemical and cytochemical evidence for ATPase activity in basal bodies isolated from oviduct. *J. Cell Biol.* 74:547–560.
- Costello, D. P., M. E. Davidson, A. Eggers, M. H. Fox, and C. Henly. 1957. Methods for Obtaining and Handling Marine Eggs and Embryos. Lancaster Press, Inc., Lancaster, Pa.
- Dewel, W. C., and W. H. Clark, Jr. 1972. An ultrastructural investigation of spermiogenesis and the mature sperm in the anthozoan *Bunodosoma cavernata* (Cnidaria). *J. Ultrastruct. Res.* 40:417–431.
- Flock, A., and A. J. Duvall. 1965. The ultrastructure of the kinocilium of the sensory cells in the inner ear and lateral line organs. *J. Cell Biol.* 25: 1–8.
- Flock, A., and J. M. Jorgenson. 1974. The ultrastructure of lateral line sense organs in the juvenile salamander *Ambystoma mexicanum*. *Cell Tissue Res.* 152:238–292.
- Goodenough, U. W., and R. L. Weiss. 1978. Interrelationships between microtubules, a striated fiber, and the gametic mating structure of *Chlamydomonas reinhardtii*. *J. Cell Biol.* 76:430–438.
- Gordon, R. E., B. P. Lane, and F. Miller. 1979. Electron microscopic localization of contractile proteins in cilia of tracheal epithelial cells. *J. Cell Biol.* 83(2), Pt. 2:176 a (Abstr.).
- Hinsch, G. W., and W. H. Clark, Jr. 1973. Comparative fine structure of cnidarian spermatozoa. *Biol. Reprod.* 8:62–73.
- Hoffman, L., and I. Manton. 1962. Observations on the fine structure of the zoospore of *Oedogonium cordiacum* with special reference to the flagellar apparatus. *J. Exp. Bot.* 13: 443–449.
- Horridge, G. A. 1964. Presumed photoreceptive cilia in a ctenophore. *Q. J. Microsc. Sci.* 105:311–317.
- Karnovsky, M. J. 1965. A formaldehyde glutaraldehyde fixative of high osmolarity for use in electron microscopy. *J. Cell Biol.* 27(2, Pt. 2):137a–138a (Abstr.).
- Kleve, M. G. 1977. The structure and function of the cnidarian (*Hydractinia echinata*) sperm centriolar complex. Doctoral Dissertation. Department of Biology, University of Houston, Houston, Tex.
- Kleve, M. G., and W. H. Clark, Jr. 1976. The structure and function of centriolar satellites and pericentriolar processes in cnidarian sperm. In *Coelenterate Ecology and Behavior*. G. O. Mackie, editor. Plenum Press, New York. 309–317.
- Kleve, M. G., J. W. Fuseler, and W. H. Clark, Jr. 1979. Antibodies against invertebrate actin: Their phylogenetic cross-reactivity. *J. Exp. Zool.* 209:21–31.
- Lazarides, E., and K. Weber. 1974. Actin antibody: the specific visualization of actin filaments in non-muscle cells. *Proc. Natl. Acad. Sci. U. S. A.* 71(6):2268–2272.
- Matsusaka, T. 1967. ATPase activity in the ciliary rootlets of human retinal rods. *J. Cell Biol.* 33:203–208.
- Miller, R. L. 1966. Chemotaxis during fertilization in the hydroid *Companularia*. *J. Exp. Zool.* 162:23–44.
- Miller, R. L. 1970. Sperm migration prior to fertilization in the hydroid *Gonothyrea lovini*. *J. Exp. Zool.* 175:493–504.
- Miller, R. L. 1972. Gel filtration of the sperm attractants of some marine hydrozoa. *J. Exp. Zool.* 182:281–298.
- Miller, R. L. 1974. Sperm behavior close to *Hydractinia* and *Ciona* eggs. *Am. Zool.* 14: 1250.
- Miller, R. L. 1975. Effect of calcium on *Tubularia* sperm chemotaxis. *J. Cell Biol.* 67:285a.
- Miller, R. L. 1976. Some observations on sexual reproduction in *Tubularia*. In *Coelenterate Ecology and Behavior*. G. O. Mackie, editor. Plenum Press, New York. 299–308.
- Miller, R. L. 1977. Chemotactic behavior of the sperm of chitons (Mollusca: *Polyplacophora*). *J. Exp. Zool.* 202:203–211.
- Miller, R. L. 1977. Distribution of sperm chemotaxis in the animal kingdom. In *Advances in Invertebrate Reproduction*. Volume 1. K. G. Adiyodi and R. G. Adiyodi, editors. Peralam-Kenoth, Karivellur, Karala, India. 99–119.
- Miller, R. L., and C. J. Brokaw. 1970. Chemotactic turning behaviour of *Tubularia* spermatozoa. *J. Exp. Biol.* 52:699–706.
- Miller, R. L., and C. Tseng. 1974. Properties and partial purification of the sperm attractant of *Tubularia*. *Am. Zool.* 14:467–486.
- Pitelka, D. R. 1974. Basal bodies and root structures. In *Cilia and Flagella*. M. A. Sleight, editor. Academic Press Inc. Ltd., London. 437–469.
- Reese, T. S. 1965. Olfactory cilia in the frog. *J. Cell Biol.* 25:209–230.
- Salisbury, J. L., and G. L. Floyd. 1978. Calcium-induced contraction of the rhizoplast of a quadraflagellate green alga. *Science (Wash. D. C.)* 202(4371):975–977.
- Simpson, P. A., and A. D. Dingle. 1971. Variable periodicity in the rhizoplast of *Naegleria* flagellates. *J. Cell Biol.* 51:323–328.
- Spudich, J. A., and S. Watt. 1971. The regulation of rabbit skeletal muscle contraction. I. Biochemical studies of the interaction of the tropomyosin-troponin complex with actin and the proteolytic fragment of myosin. *J. Biol. Chem.* 246:4866–4871.
- Spurr, A. K. 1969. A low viscosity epoxy resin embedding medium for electron microscopy. *J. Ultrastruct. Res.* 26:31–43.

33. Stephens, R. E. 1975. The basal apparatus. Mass isolation from the molluscan ciliated gill epithelium and a preliminary characterization of striated rootlets. *J. Cell Biol.* 64:408-420.
34. Summers, R. G. 1972. A new model for the structure of the centriolar satellite complex in spermatozoa. *J. Morphol.* 137:229-242.
35. Szollosi, D. 1964. The structure and function of centrioles and their satellites in the jellyfish *Phialidium gregarium*. *J. Cell Biol.* 21:465-479.
36. Talbot, P., and M. G. Kleve. 1978. Hamster sperm cross react with antiactin. *J. Exp. Zool.* 204:131-136.
37. Tokuyasu, U., and E. Yamada. 1959. The fine structure of the retina. Studies with the electron microscope. IV. Morphogenesis of outer segments of retinal rods. *J. Biophys. Biochem. Cytol.* 6:225-230.
38. Weber, K., and M. Osborn. 1969. The reliability of molecular weight determination by dodecyl sulfate-polyacrylamide gel electrophoresis. *J. Biol. Chem.* 244(16):4406-4412.
39. Wesall, J., A. Flock, and P. G. Lundquist. 1965. Structural basis for directional sensitivity in cochlear and vestibular sensory receptors. *Cold Spring Harbor Symp. Quant. Biol.* 30: 115-132.